

Fig. S1. Effects of hepatic β Klotho knockdown in HFHS diet-fed mice treated with FGF21.

(A) The β Klotho mRNA were decreased by Ad-shKLB in primary hepatocytes. shKLB-18 that produced the greatest knockdown efficiency of 75% was chosen for the following in vitro and vivo experiments. The data are represented as the mean \pm SEM, $n=3-4$. * $p<0.05$, versus cells treated with negative control shRNA. Cells were treated with adenovirus expressing short-hairpin RNA targeting β Klotho (shKLB) or negative control (shNC) for 72 h. The infection of adenovirus was confirmed by representative fluorescence of GFP (green fluorescent protein) in primary mouse hepatocytes. Hepatocytes without adenovirus infection (Blank) were used as the control. (B) shRNA-mediated β Klotho knockdown attenuated FGF21's effects on ERK1/2 signaling in primary hepatocytes. After a 48 h period of infection with adenoviruses encoding GFP, FGF21, shNC, or shKLB, primary mouse hepatocytes were incubated with serum free medium for overnight, then treated with insulin (100 nM) for 10 min before analyzed by immunoblots. (C-F) Eight-week-old male C57BL/6 mice were fed on a HFHS diet for 14 weeks, followed by injection with Ad-shKLB or Ad-shNC adenoviruses via tail-vein injection, and then treated with recombinant FGF21 (0.4 mg/kg/day) or PBS as vehicle control via subcutaneous injection once daily for 10 days. (C) Reduced expression of β Klotho in the liver of Ad-shKLB treated mice. β Klotho protein levels in livers of HFHS diet-fed mice treated with Ad-shNC and Ad-shKLB were measured by immunoblots. (D) Ad-shKLB attenuated FGF21-induced phosphorylation of ERK1/2 in the liver. Representative immunoblots for phosphorylation of ERK1/2 in the liver of Ad-shNC or Ad-shKLB treated mice. (E) Effects of FGF21 administration on liver triglyceride, plasma triglyceride and cholesterol levels. (F) Administration of FGF21 increased the transcription of adiponectin in the white adipose tissue of mice. The data are represented as the mean \pm SEM, $n=5-8$. * $p<0.05$, versus Ad-shNC and vehicle treated mice; # $p<0.05$, versus Ad-shKLB and vehicle treated mice.

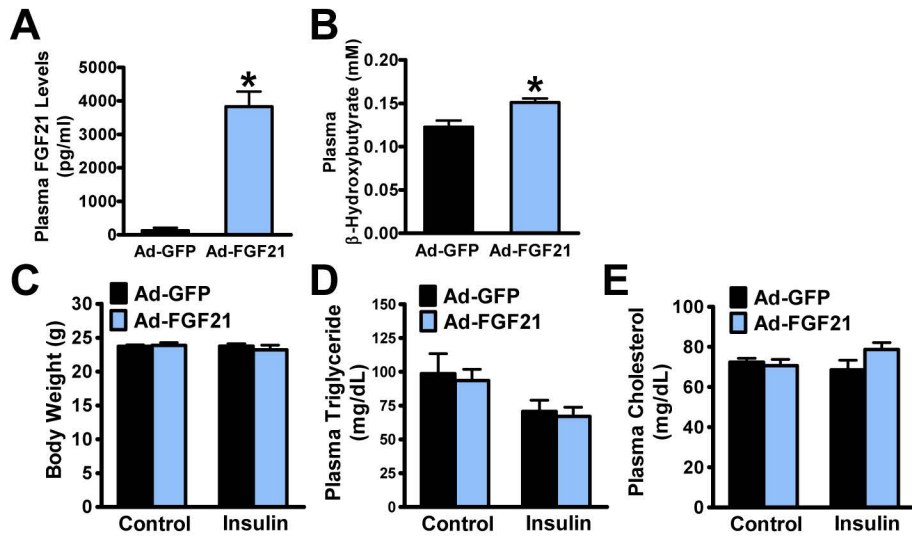


Fig. S2. Effects of adenoviral overexpression of FGF21 in mice. Eight-week-old male C57BL/6 mice were treated with FGF21 or GFP adenoviruses (5×10^9 pfu) via tail-vein injection for 2 weeks, followed by intraperitoneal injection with insulin (1 U/kg) or PBS (Control), the animals were sacrificed after 10 minutes. (A-B) Plasma levels of FGF21 (A) and β -hydroxybutyrate (B) in mice. (C) Body weight of Ad-FGF21 and Ad-GFP mice. (D-E) Plasma triglyceride (D) and cholesterol (E) levels in mice. The data are represented as the mean \pm SEM, $n=4-6$. * $p < 0.05$, versus Ad-GFP.

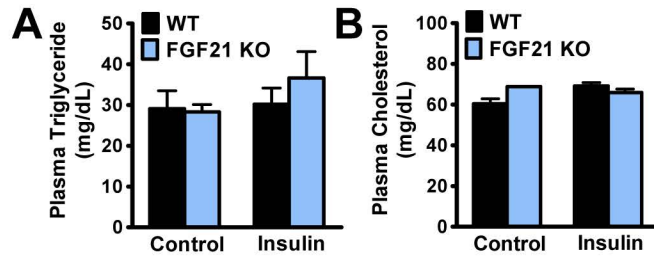


Fig. S3. Effects of FGF21 deficiency on plasma lipid levels in mice treated without or with insulin. FGF21 knockout and WT mice at 5-6 months of age were injected with Insulin or PBS (Control) intraperitoneally, the animals were sacrificed after 10 minutes. (A-B) Plasma triglyceride (A) and cholesterol (B) levels in mice. The data are represented as the mean \pm SEM, n=3.

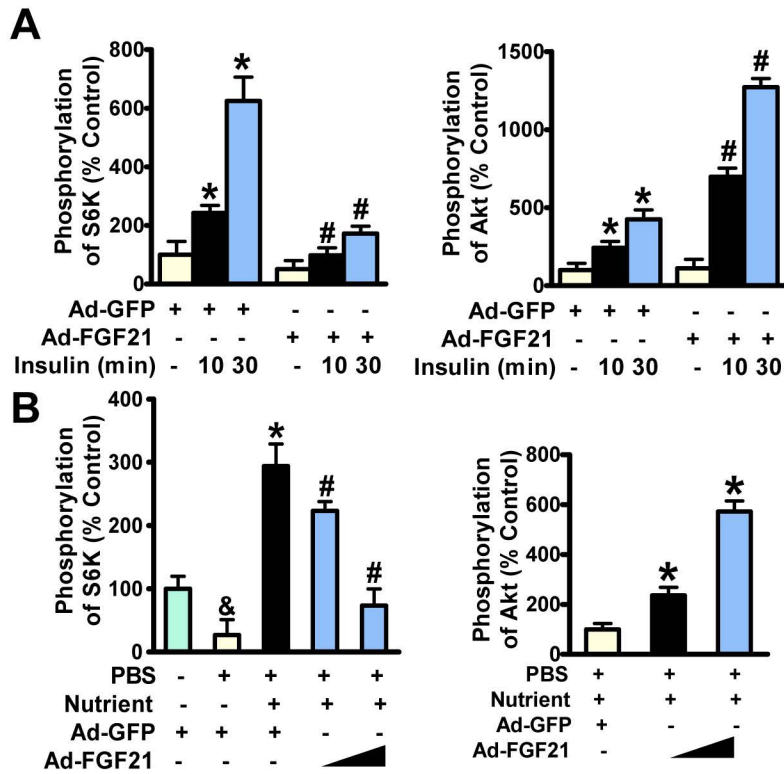


Fig. S4. Overexpression of FGF21 inhibited insulin (A)- and nutrient (B)-stimulated activation of mTORC1 to enhance phosphorylation of Akt in HepG2 cells. Representative densitometric quantification of immunoblots for phosphorylation of S6K and Akt in HepG2 cells in Fig. 5A and 5B is shown.

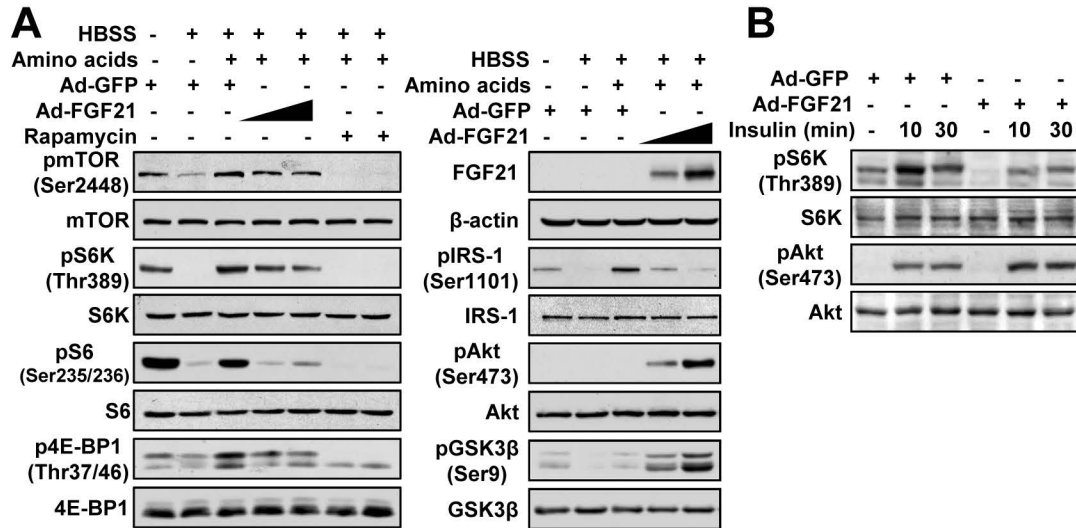


Fig. S5. FGF21 inhibits mTORC1 activation and improves insulin sensitivity in HepG2 cells. (A) Overexpression of FGF21 inhibited amino acid-stimulated activation of mTORC1 to enhance phosphorylation of Akt in HepG2 cells. Cells infected with Ad-GFP or Ad-FGF21 for 48 h were treated without or with rapamycin (5 nM) for overnight, followed by incubation with HBSS for 1 h, then treated for 30 min without or with 2Xamino acids mixture. Representative immunoblots for phosphorylation of mTOR, S6K, S6, 4E-BP1, IRS-1, Akt and GSK3 β in HepG2 cells are shown. (B) Overexpression of FGF21 inhibited insulin-stimulated activation of mTORC1 to enhance phosphorylation of Akt in Huh7 cells. Cells were infected with Ad-GFP or Ad-FGF21 for 48 h, followed by incubation in serum free medium without or with rapamycin (5 nM) for overnight, then treated for 10 or 30 min with insulin (100 nM). Representative immunoblots for phosphorylation of S6K and Akt are shown.

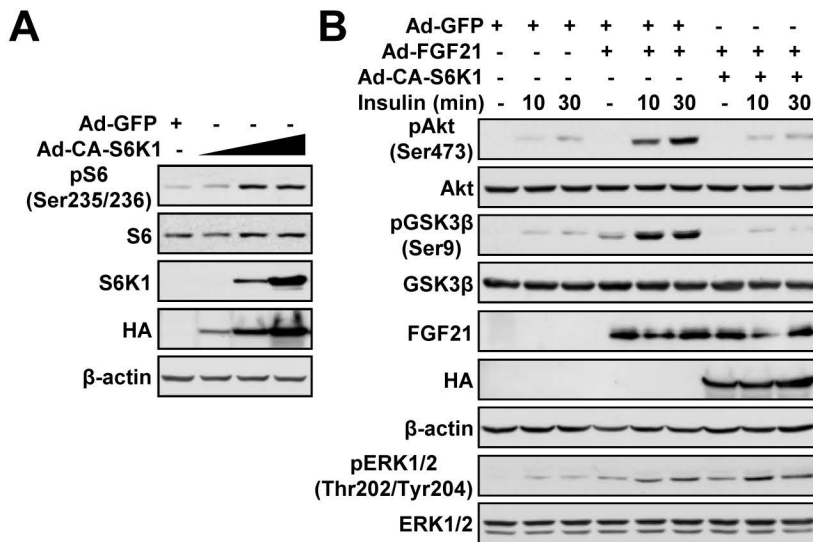


Fig. S6. mTORC1 inhibition is responsible for hepatic insulin sensitizing effects of FGF21 *in vitro*. (A-B) Constitutively activation of S6K1 abolished insulin sensitizing effects of FGF21 in HepG2 cells. (A) Expression of constitutively active S6K1 adenovirus in HepG2 cells was confirmed by immunoblots. Cells were harvested after a 72 h period of infection with Ad-GFP or a HA-tagged S6K1 (Ad-CA-S6K1). Representative immunoblots for S6K1, HA and β-actin, and phosphorylation of S6 are shown. (B) Constitutively active S6K1 abrogated FGF21's effects on insulin sensitivity in HepG2 cells. Cells were infected with Ad-GFP, Ad-FGF21, or Ad-CA-S6K1 for 48 h, followed by incubation in serum free medium for overnight, and then treated without or with insulin (100 nM) for 10 min. Representative immunoblots for phosphorylation of Akt, GSK3β and ERK1/2, and expression levels of FGF21, HA-tagged S6K1 and β-actin are shown.

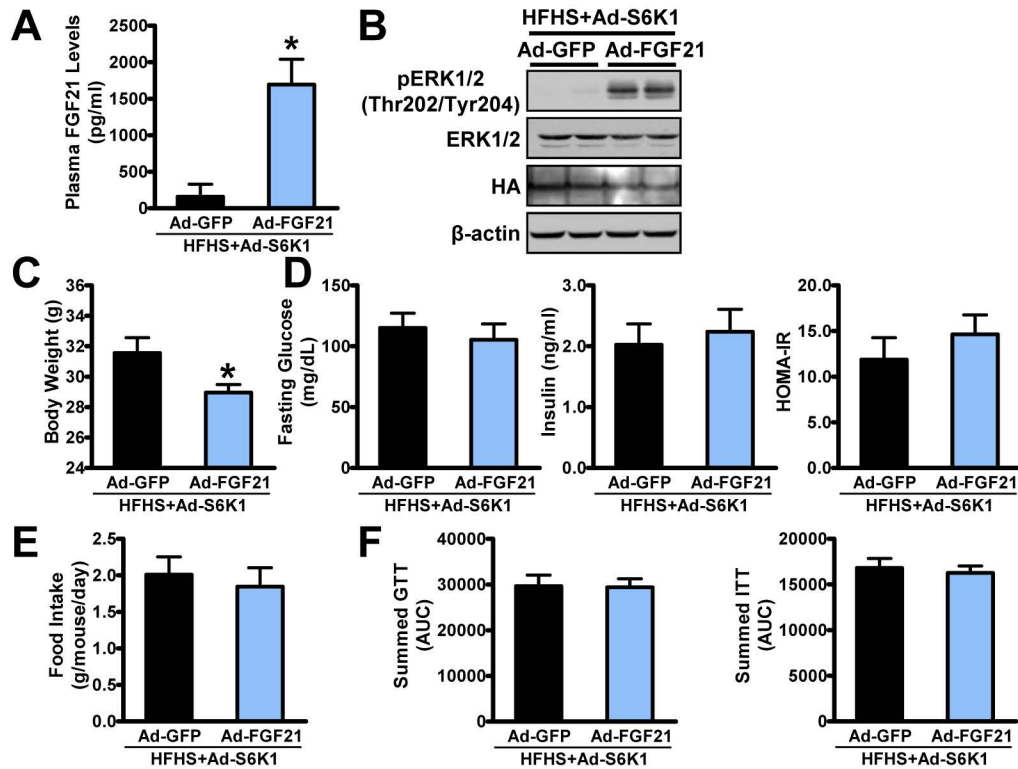


Fig. S7. FGF21's improvements in insulin sensitivity are abrogated by hepatic overexpression of S6K1 in mice. Eight-week-old male C57BL/6 mice were fed on a HFHS diet for 10 weeks, followed by treatment with constitutive active S6K1 (Ad-CA-S6K1), GFP or FGF21 adenoviruses via tail-vein injection for two weeks. (A) Plasma levels of FGF21 in mice. (B) Representative immunoblots for phosphorylation of ERK1/2, and expression levels of HA-tag and β -actin in mouse livers. (C) FGF21 reduces body weight in Ad-S6K1 treated mice fed with HFHS diet. (D) Blood glucose, plasma insulin levels, and calculated HOMA-IR were assessed. (E) Food intakes were similar between GFP- and FGF21-treated mice. (F) Summed results from GTTs or ITTs are shown. The data are represented as the mean \pm SEM, $n=4$. * $p<0.05$, versus the GFP-treated mice.

Fibroblast Growth Factor 21 Improves Hepatic Insulin Sensitivity by Inhibiting Mammalian Target of Rapamycin Complex 1

Qi Gong¹, Zhimin Hu¹, Feifei Zhang¹, Aoyuan Cui¹, Xin Chen^{4,5}, Haoyang Jiang¹, Jing Gao¹, Xuqing Chen³, Yamei Han¹, Qingning Liang^{7,8}, Dewei Ye⁸, Lei Shi², Y. Eugene Chin⁴, Yu Wang^{7,8}, Hui Xiao², Feifan Guo¹, Yong Liu¹, Mengwei Zang⁶, Aimin Xu^{7,8,9}, Yu Li^{1*}

¹Key Laboratory of Nutrition and Metabolism, Institute for Nutritional Sciences, Shanghai Institutes for Biological Sciences, Chinese Academy of Sciences, Shanghai 200031, China; ²Key Laboratory of Molecular Virology & Immunology, Institut Pasteur of Shanghai, Chinese Academy of Sciences, Shanghai 200031, China; ³College of Life and Environmental Sciences, Shanghai Normal University, Shanghai 200234, China; ⁴Institute of Health Sciences, Shanghai Institutes of Biological Sciences, Chinese Academy of Sciences, Shanghai, 200025, China; ⁵School of Life Science and Technology, ShanghaiTech University, Shanghai 200031, China; ⁶Department of Medicine, Boston University School of Medicine, Boston, Massachusetts; ⁷State Key Laboratory of Pharmaceutical Biotechnology, The University of Hong Kong, Hong Kong, China; ⁸Department of Medicine, The University of Hong Kong, Hong Kong, China; ⁹Department of Pharmacology and Pharmacy, The University of Hong Kong, Hong Kong, China;

Supplemental Experimental Procedures

Reagents and antibodies—Lyophilized mouse recombinant FGF21 (cat. 42189) that is dissolved in deionized water to prepare the working stock solution, and human FGF21 enzyme-linked immunosorbent assay kit (cat. 31180) were obtained from Antibody and Immunoassay Services at the University of Hong Kong, China. mTORC1 inhibitor rapamycin was purchased from LC Laboratories (Woburn, MA). Human recombinant insulin was from TOCRIS Bioscience (Bristol, UK). FLAG M2 monoclonal antibody, palmitic acid and tamoxifen were from Sigma-Aldrich (St. Louis, MO). Rabbit polyclonal phospho-mTOR Ser2448 (cat. 2971), phospho-S6K Thr389 (cat. 9234), phospho-S6 Ser235/236 (cat. 2211), phospho-4E-BP1 Thr37/46 (cat. 9459), Phospho-IRS-1 Ser1101 (cat. 2385), phospho-Akt Ser473 (cat. 9271), Phospho-GSK3 α/β Ser21/9 (cat. 9331), mouse polyclonal phospho-ERK1/2 Thr202/Tyr204 (cat. 9106), as well as total mTOR (cat. 2972), S6K (cat. 9202), S6 (cat. 2217), 4E-BP1 (cat. 9452), Akt (cat. 9272), ERK1/2 (cat. 9102), TSC1 (cat. 4906), and the selective ERK inhibitor U0126 (cat. 9903) were purchased from Cell Signaling Technology (Beverly, MA). Mouse monoclonal IRS-1 antibody (cat. 05-699, clone 1M92-7) was obtained from Upstate Biotechnology (Lake Placid, NY). Mouse monoclonal anti-HA (16B12) antibody was from COVANCE (Princeton, NJ). Mouse monoclonal GSK3 β antibody (cat. 610202) was from BD Biosciences (San Jose, CA). Rabbit polyclonal phospho-GS [pSpS641/645] antibody (cat. 44-1092G) and amino acids solution (50X) was from Life Technologies (Grand Island, NY). Polyclonal FGF21 antibody (cat. AF3057) was from R&D Systems (Minneapolis, MN). Mouse monoclonal anti-HA (16B12) antibody was from COVANCE (Princeton, NJ). Mouse monoclonal GS (G-8) (cat. sc-390391), β Klotho (cat. sc-74343), β -actin (cat. sc-69879) antibodies, and horseradish peroxidase-conjugated anti-mouse, anti-rabbit and anti-goat secondary antibodies were obtained from Santa Cruz Biotechnology (Santa Cruz, CA).

Animal model and diets—Mice were fed on high-fat, high-sucrose diet (D12327, Research Diets) for 10-14 weeks, followed by injection with adenoviruses via tail-vein injection, and then treated without or with recombinant FGF21 or PBS as vehicle control via subcutaneous injection once daily for 10 days. For nonalcoholic steatohepatitis mouse model, mice were fed on methionine- and choline-deficient (MCD) diet (A02082002B, Research Diets) for 3 weeks, and then treated without or with recombinant FGF21 or PBS as vehicle control via subcutaneous injection once daily for 10 days. For *in vivo* insulin signaling assay, the mice were intraperitoneally injected with insulin (1 U/kg) or PBS for 10 min, and then sacrificed and tissues were rapidly collected. All mice were housed under a 12:12-h light/dark cycle at controlled temperature.

Histological analysis of the NASH CRN Score—NASH CRN Score were evaluated according to the NASH Clinical Research Network (CRN) scoring system as described previously(1, 2). The NAS scores ranging from 0 to 8 were defined as the sum of the scores for steatosis (0-3): 0<5%, 1: 5-33%, 2: 34-66%, 3: >66%; lobular inflammation (0-3): 0: none, 1: <2 foci/20x field, 2: 2-4 foci/20x field, 3: >4 foci/20x field; hepatocellular ballooning (0-2): 0: none, 1: mild/few; 2: moderate-marked/many.

Measurement of blood glucose, plasma and liver lipids, FGF21 and β -hydroxybutyrate, and food intake—Blood glucose concentrations were determined by AlphaTRAK Glucose Meter (Abbott Laboratories, IL). Plasma insulin levels were measured using Mercodia Ultrasensitive Mouse Insulin ELISA (Uppsala, Sweden). The homeostasis model assessment of insulin resistance (HOMA-IR) was calculated as previously described(3, 4): $\text{HOMA-IR} = \frac{\text{plasma glucose concentration (in mmol/l)} \times \text{plasma insulin concentration (in } \mu\text{U/ml)}}{22.5}$. Plasma and liver triglyceride and cholesterol levels were analyzed as previously described(4). Briefly, liver tissues were homogenized in PBS, and then extracted using chloroform/methanol (2:1), dried

under nitrogen gas and then resuspended in isopropanol. Infinity Triglycerides kit (cat. TR22421) and Total Cholesterol kit (cat. TR13421) obtained from Stanbio Laboratory (Boerne, TX) were used for the measurement of plasma and liver lipids. Measurements of liver lipids were normalized to those of protein concentrations in the initial homogenate as determined by protein quantification. The Quantikine Mouse FGF21 enzyme-linked immunosorbent assay kit (cat. MF2100) was from R&D Systems (Minneapolis, MN). The β -hydroxybutyrate LiquidColor Test kit (catalog no. 2440-58) was from Stanbio Laboratory (Boerne, TX). Food intake was measured as described previously⁽⁵⁾. Briefly, food intake of each individual mouse was recorded daily for 1 week after 3 days of adaptation. During each 24-hour period, each mouse was housed with a thin layer of bedding, and a known quantity of diet was provided. After 24 hours, the remaining food was weighed.

Liver glycogen measurement—Mouse liver glycogen was measured by Glycogen Colorimetric/Fluorometric Assay Kit (BioVision, CA). The liver glycogen is hydrolyzed to glucose by glucoamylase, which is then specifically oxidized to produce a product that reacts with OxiRed probe to generate color at OD 570 nm. Briefly, mouse liver tissues were homogenized with dH₂O on ice. The homogenates were boiled for 10 min to inactivate enzymes, followed by centrifugation at 18000 x g for 10 min. The supernatant was mixed with hydrolysis buffer and hydrolysis enzyme mix in a 96-well plate, and then incubated for 30 min at room temperature. The reaction mix containing development buffer, development enzyme mix and OxiRed probe was added into each well. Then the reaction was incubated for 30 min at room temperature, protected from light, prior to measurement of absorbance at 570 nm. Mouse liver glycogen concentrations were calculated according to the standard curve, and normalized to the liver weight.

Glucose-tolerance tests (GTTs) and insulin-tolerance tests (ITTs)—GTTs and ITTs were performed as described previously(6). For GTTs, mice were deprived of food for 16 h, and then were injected with glucose solution (1 g/kg body weight) intraperitoneally. Blood glucose was measured 0, 15, 30, 60, 90, and 120 min after glucose injection. For ITTs, mice were deprived of food for 6 h, and then were injected with short-acting human insulin (0.75 U/Kg, Eli Lilly). Blood glucose was measured 0, 15, 30, 60, 90, and 120 min after insulin injection.

Plasmid construction and transfection—The lentiviral transfer plasmid encoding FLAG-tagged human RagA was constructed by amplifying PCR products from cDNA library generated from HEK293T cells, and inserting it into the XbaI/BamHI site of the lentiviral transfer vector pLVX-IRES-Puro. Then the pLVX-IRES-Puro-FLAG-RagA^{Q66L} mutant was created using the QuickChange Site-Directed Mutagenesis Kit (Stratagene, La Jolla, CA) and the following primers: TGGGACTGTGGCGGTCTGGACACCTTCATGGA (F) and TCCATGAAGGTGTCCAGACCGCCACAGTCCCAC (R). Mutated bases were indicated by underlining. All constructs and mutations were verified by sequencing. Transfection assays for plasmids or siRNAs were performed using Lipofectamine 2000 (Life Technologies) according to the manufacturer's protocol.

Primary mouse hepatocyte isolation and culture—Primary mouse hepatocytes were isolated using a method described previously(4, 7). Briefly, mice were anesthetized with sodium pentobarbital (30 mg/kg intraperitoneally), and the portal vein was cannulated under aseptic conditions. The liver was perfused with ethylene glycol-bis(2-aminoethylether)-N,N,N',N'-tetraacetic acid (EGTA) solution (5.4 mmol/l KC1, 0.44 mmol/l KH₂PO₄, 140 mmol/l NaCl, 0.34 mmol/l Na₂HPO₄, 0.5 mmol/l EGTA, 25 mmol/l Tricine, pH 7.2) and Gey's Balanced Salt Solution (GBSS) containing 0.075% collagenase

type I (Sigma-Aldrich), 10mg/ml DNase I (Sigma-Aldrich), 200 units/ml penicillin, and 200 µg/ml streptomycin, and then digested with 0.025% collagenase solution for the mouse liver. The isolated mouse hepatocytes were then cultured at 80%-90% confluence in DMEM medium containing 10% FBS in rat-tail collagen type I-coated 6-well plates (BD Biosciences) for overnight. Cells were infected with adenoviruses expressing FGF21 or GFP, treated without or with rapamycin in a serum free medium, and then treated with insulin as indicated.

Immunoblotting analysis—Immunoblotting analysis was carried out as described previously(4, 5).

In brief, mouse liver tissues or cultured cells were homogenized and lysed at 4 °C in lysis buffer (50 mM Tris-HCl, pH 8.0, 1% (v/v) Nonidet P-40, 150 mM NaCl, 5 mM EDTA, 1 mM EGTA, 1 mM sodium orthovanadate, 10 mM sodium fluoride, 1 mM phenylmethylsulfonyl fluoride, 2 µg/ml aprotinin, 5 µg/ml leupeptin, and 1 µg/ml pepstatin). Cell lysates were centrifuged at 14,000 rpm for 10 min at 4 °C, and the resulting supernatant was used for immunoblotting analysis. Protein concentrations in cell lysates were measured using Bio-Rad Protein Assay Dye Reagent. For immunoblotting, 20–50 µg of protein were separated by 8-10% sodium dodecyl sulfate-polyacrylamide gel electrophoresis (SDS-PAGE), and then electrophoretically transferred to polyvinylidene difluoride (PVDF) membranes in a transfer buffer consisting of 25 mM Tris base, 190 mM glycine, and 20% methanol. The membranes were blocked with 5% non-fat milk in Tris-buffered saline with 0.1% Tween 20 (TBST) and incubated with specific antibodies, followed by incubation with horseradish peroxidase-conjugated secondary antibodies. Immunoblots were visualized by LumiGLO chemiluminescence detection kit (Cell Signaling Technology). The intensity of bands was quantified using ImageJ (National Institutes of Health, Bethesda, MD). Relative phosphorylation levels were normalized to those of endogenous proteins and presented as the means±SEM.

D-[³H]Glycogen synthesis assay. Glycogen synthesis was determined using a modified method described previously(8). Primary mouse hepatocytes seeded in 24-well plates were treated as required, followed by glycogen synthesis assay. Cells were washed twice with serum free DMEM with low glucose (1.0 g/L), and then incubated in 1 μ Ci/ml D-[³H]glucose (PerkinElmer) without or with 100 nM insulin in DMEM for 3h. The labeling media was aspirated, and then cells were lysed in 200 μ l 0.2 N KOH containing 5 mg/ml glycogen at 60°C for 30 min. The cell lysates were transferred to 1.5 ml tubes, and the incubation was continued at 60°C for 1h. The tubes were chilled on ice for 2 min, and 1 ml of cold ethanol (-20°C) was added, and then followed by centrifugation at 5000 \times g for 5 min to separate glycogen. The pellets were washed twice with 1ml of cold ethanol, and then solubilized in 200 μ l of 0.2 N HCl and measured by a Beckman LS6500 Liquid Scintillation Counter by adding 0.7 ml of high-flashpoint scintillation cocktail. The glycogen synthesis activities were normalized to proteins concentrations in duplicates of a 24-well plate with the same treatment conditions, and presented as relative glycogen synthesis.

Generation of adenoviruses expressing FGF21 and constitutive active S6K1—Adenoviruses expressing mouse FGF21 and constitutive active S6K1 (CA-S6K1) were generated using the AdEasy system as described previously(5, 6, 9, 10). The cDNAs encoding mouse FGF21 and HA-tagged constitutive active rat S6K1(11) that was cloned from an expressing plasmid obtained from Addgene (cat. 8991, Cambridge, MA) were cloned into the shuttle vector pShuttle-CMV. The resultant plasmid was purified using phenol/chloroform and linearized by the restriction endonuclease PmeI and used to transform the E. coli strain BJ5183-AD1 competent cells (Agilent Technologies) containing the supercoiled adenoviral vector pAd-Easy1 by electroporation (2.5kV, 200 ohms, 25 μ F). Recombinant bacteria colonies were selected by kanamycin resistance and

screened by restriction endonuclease *PacI* digestion to release a 4.5kb or 3 kb fragment together with a 35kb adenovirus vector fragment. Then, the recombinant adenoviral construct was purified using phenol/chloroform and linearized with *PacI*, then used to transfect the packaging cell line HEK293A with Lipofectamine 2000 (Life Technologies) and harvest the cells around seven days post-transfection to produce adenovirus. The cells and cultured media were harvested, and virus is released by three freeze-thaw cycles alternately using a 37 °C water bath and liquid nitrogen. Then, adenoviruses were propagated in HEK293A. Briefly, cells were infected with the adenovirus at a confluency of approximately 80% in DMEM supplemented with 4% fetal bovine serum, and the cells and cultured media were harvested 2-3 days post-infection when most of the infected cells were rounded up. Virus is released by three freeze-thaw cycles of the infected HEK293A cells alternately using a 37 °C water bath and liquid nitrogen. The virus was purified by Adenopure adenovirus purification Kit (Puresyn, Malvern, PA).

Lentiviral particles production—Lentiviral particles were generated using a modified method as described previously(12). Briefly, HEK293T cells were cotransfected with 1 µg of lentiviral transfer plasmid pLVX-IRES-Puro-FLAG-RagA^{Q66L}, along with 650 ng of packaging plasmid psPAX2, and 350 ng of envelope plasmid pMD2.G in a 6-cm plate using Lipofectamine 2000 (Life Technologies). Twelve hours post transfection, the media was changed, and cells were cultured in 5 ml fresh DMEM containing 10% fetal bovine serum, 100 units/ml penicillin, and 100 µg/ml streptomycin. Twenty four hours post incubation, the media that containing lentiviral particles was harvested and stored at 4 °C. The resulting cells were cultured in 5 ml fresh DMEM containing 10% fetal bovine serum, 100 units/ml penicillin, and 100 µg/ml streptomycin, and then incubated for additional 24 hours. The

media was then harvested and pooled with the media harvested in the previous day. The pooled media containing lentiviral particles was filtered through a 0.45 μm filter and then stored at 4 °C.

Lentiviral particles infection and selection—For lentivirus infection, cells were cultured to approximately 70% confluent. Then the media was changed, and cells were cultured in fresh media containing 8 $\mu\text{g}/\text{mL}$ polybrene, followed by adding lentiviral particle solution to the media. Twenty-four hours post infection, the media was changed, and cells were selected and passaged under puromycin-containing media for 4-7 days. The resulting cells were ready for further assays.

Cell treatment—Primary mouse hepatocytes, and human HepG2 and Huh7 hepatocytes were cultured and treated as described previously(4, 5, 13). Cells were cultured in DMEM containing 5.5 mM D-glucose, 10% fetal bovine serum, 100 units/ml penicillin, and 100 $\mu\text{g}/\text{ml}$ streptomycin, and incubated in a humidified atmosphere of 5% CO_2 at 37 °C and passaged every 2 days by trypsinization. For insulin-induced mTORC1 activation, cells were infected with Ad-GFP or Ad-FGF21 for 48 h, followed by incubation in serum free medium for overnight, and then treated with insulin (100 nM) for 10 or 30 min. Nutrient- or amino acid-stimulated activation of mTORC1 signaling was described previously(14-16). Briefly, after serum starvation for overnight, cells were incubated in PBS or HBSS for 1h, and then treated with DMEM containing 10% FBS or 2X amino acids mixture for 30 min, respectively. Amino acid free (-AA) media that was used to potentiate the stimulatory effects of constitutive active Rag mutant RagA^{Q66L} on mTORC1 activation in HepG2 cells was made using DMEM medium (Life Technologies, cat. 11965) formulation as described previously(17). Briefly, inorganic salts (2X) and other components (2X) were made individually as stocks. Then inorganic salts (2X), MEM vitamin (100X, Life Technologies) and other components (2X) were mixed together with double-distilled water to bring the final concentration to 1X, 4X, and 1X, respectively. The final

pH was adjusted to 7.0-7.4. For fatty acid treatment, cells were treated with 100 μ M palmitate-BSA or control BSA for 16 h.

Fatty acid preparation—Palmitate-BSA was prepared using a modified method described previously (18, 19). Palmitic acid was dissolved in 0.1 M NaOH solution at 90 °C for 10 min. Fatty acid-free BSA was dissolved in ddH₂O and incubated at 55 °C for 20 min. The palmitate was mixed with BSA to make 10 mM palmitate-BSA stock solution, and then filtered and stored at -20 °C. Control BSA solution was prepared by mixing 0.1 M NaOH with BSA.

Tamoxifen-induced deletion of TSC1 in hepatocytes—Administration of a two-dose of tamoxifen induction was performed to delete TSC1 in the isolated hepatocytes derived from TSC1 floxed mice. The hepatocytes were cultured at 80-90% confluence in DMEM medium containing 10% FBS in rat-tail collagen type I-coated 6-well plates (BD Biosciences) for overnight. Cells were cultured in fresh DMEM containing tamoxifen (10 nM) or vehicle control, and then infected with adenovirus expressing FGF21 or GFP for overnight, followed by treatment with the second dose of tamoxifen (10 nM) or vehicle. Twenty four hours post induction, the media was changed and cells were maintained in serum free DMEM containing 5.5 mM glucose for overnight and treated with insulin (100 nM) as indicated.

RNA isolation and quantitative RT-PCR analysis—Liver tissues were homogenized in TRIzol Reagent (Life Technologies) to extract total RNAs according to the manufacturer's protocol. Total RNAs were then reversely transcribed to cDNA using SuperScript II reverse transcriptase (Life Technologies) and Oligo d (T). The resulting cDNA was subjected to real-time PCR with gene-specific primers in the presence of SYBR Green PCR master mix (Applied Biosystems) using StepOnePlus Real-Time PCR System (Applied Biosystems) as described previously(4). The

specificity of the PCR amplification was verified by analyzing the melting curve, and also by running products on an agarose gel. Data were analyzed using the $\Delta\Delta CT$ threshold cycle method. The mRNA levels of genes were normalized to those of β -actin and presented as relative levels to control. Primers were designed using Primer3 (v. 4.0).

Fluorescence microscopy—Fluorescence microscopies were performed to determine infection efficiency of adenovirus expressing shRNAs in primary hepatocytes. Cells were seeded onto glass coverslips. Seventy two hours post infection, cells were fixed in 4% paraformaldehyde and coverslips were mounted in ProLong Gold antifade reagent with DAPI (Life Technologies) to visualize the nuclei. Images were captured under a fluorescence microscope (Olympus BX53).

Reference

1. Kleiner DE, Brunt EM, Van Natta M, Behling C, Contos MJ, Cummings OW, et al. Design and validation of a histological scoring system for nonalcoholic fatty liver disease. *Hepatology*. 2005;41(6):1313-21.
2. Ye D, Li FYL, Lam KSL, Li H, Jia W, Wang Y, et al. Toll-like receptor-4 mediates obesity-induced non-alcoholic steatohepatitis through activation of X-box binding protein-1 in mice. *Gut*. 2012 July 1, 2012;61(7):1058-67.
3. Huang W, Dedousis N, O'Doherty RM. Hepatic steatosis and plasma dyslipidemia induced by a high-sucrose diet are corrected by an acute leptin infusion 2007.
4. Li Y, Xu S, Mihaylova MM, Zheng B, Hou X, Jiang B, et al. AMPK Phosphorylates and Inhibits SREBP Activity to Attenuate Hepatic Steatosis and Atherosclerosis in Diet-Induced Insulin-Resistant Mice. *Cell Metabolism*. 2011;13(4):376-88.
5. Li Y, Wong K, Giles A, Jiang J, Lee JW, Adams AC, et al. Hepatic SIRT1 Attenuates Hepatic Steatosis and Controls Energy Balance in Mice by Inducing Fibroblast Growth Factor 21. *Gastroenterology*. 2014;146(2):539-49.e7.
6. Li Y, Xu S, Giles A, Nakamura K, Lee JW, Hou X, et al. Hepatic overexpression of SIRT1 in mice attenuates endoplasmic reticulum stress and insulin resistance in the liver. *The FASEB Journal*. 2011 May 1, 2011;25(5):1664-79.
7. Radaeva S, Jaruga B, Hong F, Kim WH, Fan S, Cai H, et al. Interferon- α activates multiple STAT signals and down-regulates c-Met in primary human hepatocytes. *Gastroenterology*. 2002;122(4):1020-34.
8. Sun C, Zhang F, Ge X, Yan T, Chen X, Shi X, et al. SIRT1 Improves Insulin Sensitivity under Insulin-Resistant Conditions by Repressing PTP1B. *Cell Metabolism*. 2007;6(4):307-19.

9. Li Y, Wong K, Walsh K, Gao B, Zang M. Retinoic Acid Receptor β Stimulates Hepatic Induction of Fibroblast Growth Factor 21 to Promote Fatty Acid Oxidation and Control Whole-body Energy Homeostasis in Mice. *Journal of Biological Chemistry*. 2013 April 12, 2013;288(15):10490-504.
10. Xiao F, Huang Z, Li H, Yu J, Wang C, Chen S, et al. Leucine Deprivation Increases Hepatic Insulin Sensitivity via GCN2/mTOR/S6K1 and AMPK Pathways. *Diabetes*. 2011 March 1, 2011;60(3):746-56.
11. Holz MK, Blenis J. Identification of S6 Kinase 1 as a Novel Mammalian Target of Rapamycin (mTOR)-phosphorylating Kinase. *Journal of Biological Chemistry*. 2005 July 15, 2005;280(28):26089-93.
12. Dull T, Zufferey R, Kelly M, Mandel RJ, Nguyen M, Trono D, et al. A Third-Generation Lentivirus Vector with a Conditional Packaging System. *Journal of Virology*. 1998 November 1, 1998;72(11):8463-71.
13. Chavez-Tapia NC, Rosso N, Tiribelli C. Effect of intracellular lipid accumulation in a new model of non-alcoholic fatty liver disease. *BMC Gastroenterology*. [journal article]. 2012;12(1):1-10.
14. Inoki K, Li Y, Zhu T, Wu J, Guan K-L. TSC2 is phosphorylated and inhibited by Akt and suppresses mTOR signalling. *Nat Cell Biol*. [10.1038/ncb839]. 2002;4(9):648-57.
15. Tremblay F, Brule S, Hee Um S, Li Y, Masuda K, Roden M, et al. Identification of IRS-1 Ser-1101 as a target of S6K1 in nutrient- and obesity-induced insulin resistance. *Proceedings of the National Academy of Sciences*. 2007 August 28, 2007;104(35):14056-61.
16. Tremblay F, Krebs M, Dombrowski L, Brehm A, Bernroider E, Roth E, et al. Overactivation of S6 Kinase 1 as a Cause of Human Insulin Resistance During Increased Amino Acid Availability. *Diabetes*. 2005 September 1, 2005;54(9):2674-84.
17. Kim E, Goraksha-Hicks P, Li L, Neufeld TP, Guan K-L. Regulation of TORC1 by Rag GTPases in nutrient response. *Nat Cell Biol*. [10.1038/ncb1753]. 2008;10(8):935-45.
18. Kwon B, Querfurth HW. Palmitate activates mTOR/p70S6K through AMPK inhibition and hypophosphorylation of raptor in skeletal muscle cells: Reversal by oleate is similar to metformin. *Biochimie*. 2015;118:141-50.
19. Ye L, Varamini B, Lamming DW, Sabatini DM, Baur JA. Rapamycin has a biphasic effect on insulin sensitivity in C2C12 myotubes due to sequential disruption of mTORC1 and mTORC2. *Frontiers in Genetics*. [Original Research]. 2012 2012-September-11;3.

Table S1. Quantitative RT-PCR primers

| Gene | Species | Forward primer | Reverse primer |
|----------------|----------------|--------------------------|-----------------------|
| FGF21 | mouse | CTGGGGGTCTACCAAGCATA | CACCCAGGATTTGAATGACC |
| β Klotho | mouse | GATGAAGAATTTCTAAACCAGGTT | AACCAAACACGCGGATTTTC |
| Adiponectin | mouse | GTTGCAAGCTCTCCTGTTCC | ATCCAACCTGCACAAGTTCC |
| β -actin | mouse | CCACAGCTGAGAGGGAAATC | AAGGAAGGCTGGAAAAGAGC |